Ferroelectrics, piezoelectric, and Impedance spectroscopy characterizations of CuO doped (Na0.52K0.44)(Nb0.9 Sb0.06)O3–0.04LiTaO3 lead free ceramics

M. Saidi, K. Khalfaoui, Ahcène Chaouchi, Sophie d'Astorg, Mohamed Rguiti, Christian Courtois

Ferroelectrics, Piezoelectric, and Impedance Spectroscopy Characterizations of CuO Doped $(Na_{0.52}\ K_{0.44})(Nb_{0.9}\ Sb_{0.06})O_3$ –0.04$LiTaO_3$ Lead Free Ceramics

M. SAIDI,[1] K. KHALFAOUI,[1] A. CHAOUCHI,[1,*]
S. D'ASTORG,[2,3] M. RGUITI,[2,3] AND C. COURTOIS[2]

[1]Laboratoire de Chimie Appliquée et Génie Chimique de l'Université Mouloud Mammeri de Tizi-Ouzou, Algérie
[2]Laboratoire des Matériaux Céramiques et Procédés Associés–Université de Valenciennes et du Hainaut-Cambrésis, Z.I. du Champ de l'Abbesse, 59600 Maubeuge, France
[3]Univ. Lille Nord de France, F-59000, Lille, France

CuO was used to reduce the sintering temperature of *$(Na_{0.52}\ K_{0.44})(Nb_{0.9}\ Sb_{0.06})O_3$ –0.04$LiTaO_3$ (NKNSLT) piezoelectric ceramics. XRD analysis reveals the formation of single phase perovskite structure. SEM has been used to investigate the grain morphology of the material. Impedance plots have been used as a tool to analyze the electrical properties of the sample as a function of frequency and temperature. Detailed studies of dielectric properties of the compound as a function of temperature at different frequencies suggest that the compound has a dielectric anomaly of ferroelectric to paraelectric type at 360°C, and exhibits diffuse phase transition. The Nyquist plot (Z' vs Z'') revealed the presence only of the grain boundary effect in the materials. Bulk resistance is observed to decrease with an increase in temperature showing a typical negative temperature coefficient of resistance (NTCR). The plot of normalized complex dielectric modulus a function of frequency exhibits both short and long-range conduction in the ceramics. The ac conductivity spectrum was found to obey Jonscher's universal power law.*

Keywords $(Na_{0.52}\ K_{0.44})(Nb_{0.9}\ Sb_{0.06})O_3$; low sintering; lead-free ceramics; dielectric properties; AC impedance spectroscopy; dielectric relaxation; conductivity

1. Introduction

The perovskite oxides were found to be useful for some solid state electronic devices such as random access memory devices, high dielectric constant capacitor, pyro-electric detectors, imaging devices, electro–optic devices, modulators etc. [1, 2]. Among the studied ferroelectric oxides, some lead based ferroelectric oxides such as lead titanate, lead

*Corresponding author; E-mail: ahchaouchi@yahoo.fr

zirconium titanate etc. are found to be most suitable for fabrication of various solid state devices. Unfortunately, because of the toxic nature they produce environmental pollutions [3]. Therefore, attempts are now being made to search lead free new ferroelectric materials which can be replacement of lead based ferroelectrics without losing much of their physical properties required for devices.

For this purpose, $(Na_{0.5}K_{0.5})NbO_3$ (NKN) based lead-free piezoelectric ceramics, based on their good dielectric, piezoelectric and electromechanical properties, and relatively high Curie temperatures. Particularly, the (Li, Ta, Sb) substituted NKN ceramics exhibit significantly improved piezoelectric properties such that they have been expected as a typical candidate to replace conventional lead-based piezoelectric ceramics [4–9].

However, the fabrication of these ceramics is very difficult because: firstly, the high hygroscopicity potassium carbonate. Secondly, the temperature stability of these ceramics is so bad because it have lower orthorhombic-tetragonal transition temperature ($T_{o\text{-}t}$). Thirdly, it is very difficult to obtain fully densified ceramics due to the evaporation of potassium during the sintering process [10–14]. Therefore, a number of studies have been carried out to improve the sinterability and then the piezoelectric properties of $(Na,K)NbO_3$ ceramics, maintaining higher orthorhombic-tetragonal transition temperature for good temperature stability of the electrical properties [15]; these include the formation of solid solutions of NKN-$SrTiO_3$ and NKN-$LiTaO_3$, and the use of sintering aids, e.g., $K_4CuNb_8O_{23}$, MnO_2, CuO, and Bi_2O_3 [16, 15].

Among them, it is well known that the CuO is good sintering aid for low temperature sintering of $(Na,K)NbO_3$-based ceramics as well as shifting the tetragonal-orthorhombic phase transition toward higher temperature. In addition, it is also a helpful sintering aid to greatly promote the densification of NKN based on the formation of liquid phases during sintering [17]. Although the addition of a small amount of CuO greatly enhances Q_m and improves densification of NKN ($\rho \simeq 98\%$ theoretical density), the d_{33} value remains low (mostly $<$100 pC/N).

Furthermore, many compositions that possess different Curie temperatures, a broad range of electrical properties and have their own morphotropic phase boundaries (MPB), can be produced by changing the ratio of Li to Ta or Sb within the NKN systems. Particularly, the textured (Li, Ta, Sb)-modified NKN ceramics exhibit piezoelectric properties comparable to those of a hard PZT [18].

It is well known that the interior defects such as A-site vacancies, space charge electrons or oxygen vacancies have great influence on ferroelectric fatigue or ionic conductivity of the material [19–21]. Considering that the solid defects play a decisive role in all of these applications, we find that it is very important to gain a fundamental understanding of their conductive mechanism. Various kinds of defects are always suggested as being responsible for the dielectric relaxations at high temperature range. The ac impedance analysis is a powerful means to separate out the grain boundary and grain-electrode effects, which usually are the sites of trap for defects. It is also useful in establishing its relaxation mechanism by appropriately assigning different values of resistance and capacitance to the grain and grain boundary effects.

In this work, CuO was used to reduce the sintering temperature of $(Na_{0.52}\ K_{0.44})(Nb_{0.9}\ Sb_{0.06})O_3$–$0.04LiTaO_3$ piezoelectric ceramics, and a detailed analysis of ac impedance spectroscopy has been carried out to characterize the dielectric, electric and conductivity properties in order to gain insight into the relaxation mechanism and defects relation.

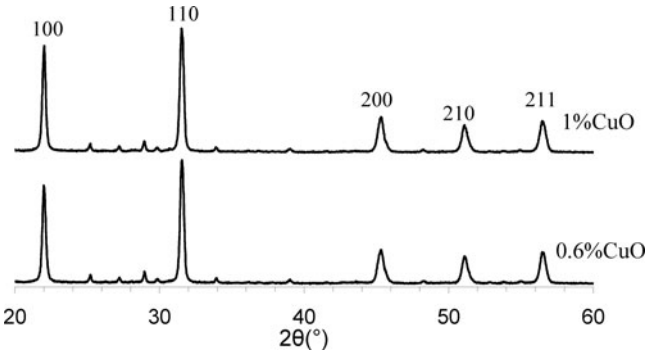

Figure 1. X-ray diffraction patterns of NKNSLT +xwt.% CuO sintered ceramics sintered at 950°C.

2. Experimental

The $(Na_{0.52}\ K_{0.44})(Nb_{0.9}\ Sb_{0.06})O_3$–$0.04LiTaO_3$ (NKNSLT) compound was prepared by solid state reaction using reagent grades powders of Na_2CO_3, Sb_2O_3, K_2CO_3, Li_2CO_3, Nb_2O_5, and Ta_2O_5 (purity >99%). These compounds were stoichiometrically mixed using isopropanol and zircon balls in a Teflon jar for 2 hours. The slurry was subsequently dried and the powder was manually reground and heat treated at 850°C for 2 hours in air. The powder was finally reground using the same process than before in isopropanol for 2 hours.

The mixtures NKNSLT +xwt.%CuO (with x = 0.6, and 1) were prepared by mixing the powders manually in porcelain mortar. To manufacture pellets, an organic binder (Polyvinyl alcohol, 5 vol%) was manually added to the powder and disks (7 and 13 mm in diameter, 1.5 mm and 1mm thickness, respectively) were shaped by uni-axial pressing under 100MPa. The green samples were finally sintered in air at 1080°C for 2 hours, with heating and cooling rates of 150°C/h. The crystallised phase composition has been identified by X-ray diffraction (XRD) technique using the Cukα X-ray radiation (Philips X' Pert) and the microstructures were observed using a scanning electron microscope (SEM Philips XL'30). The specimens were polished and electroded with a silver paste. The dielectric and electric properties was determined using HP4284A meter versus temperature (from 20°C to 500°C), and the frequency range from 100 Hz to 1 MHz. For piezoelectric measurements, the specimens were polled in a silicone oil bath under different poling. The piezoelectric coefficient (d_{33}) was measured using a piezoelectric d_{33} meter (Piezotest PM 200) at a frequency of 100 Hz. P-E hysteresis loops were obtained using Radiant Precision Workstation ferroelectric testing system.

3. Results and Discussions

3.1. Phase Analysis and Microstructure

Fig. 1 shows the XRD results of CuO doped NKNSLT ceramics. All the XRD patterns of the ceramics are single phase. The diffraction peaks shift toward a higher angle with the increase of the copper addition, which indicates the decrease of lattice constant. Their decrease is due to the incorporation of Cu^{2+} into the B-site [22].

Fig. 2 shows the SEM micrographs of the NKNSLT +xw.%CuO (with x = 0.6, and 1) ceramics. Even though the sintering temperature is as low as 950°C, the ceramics can

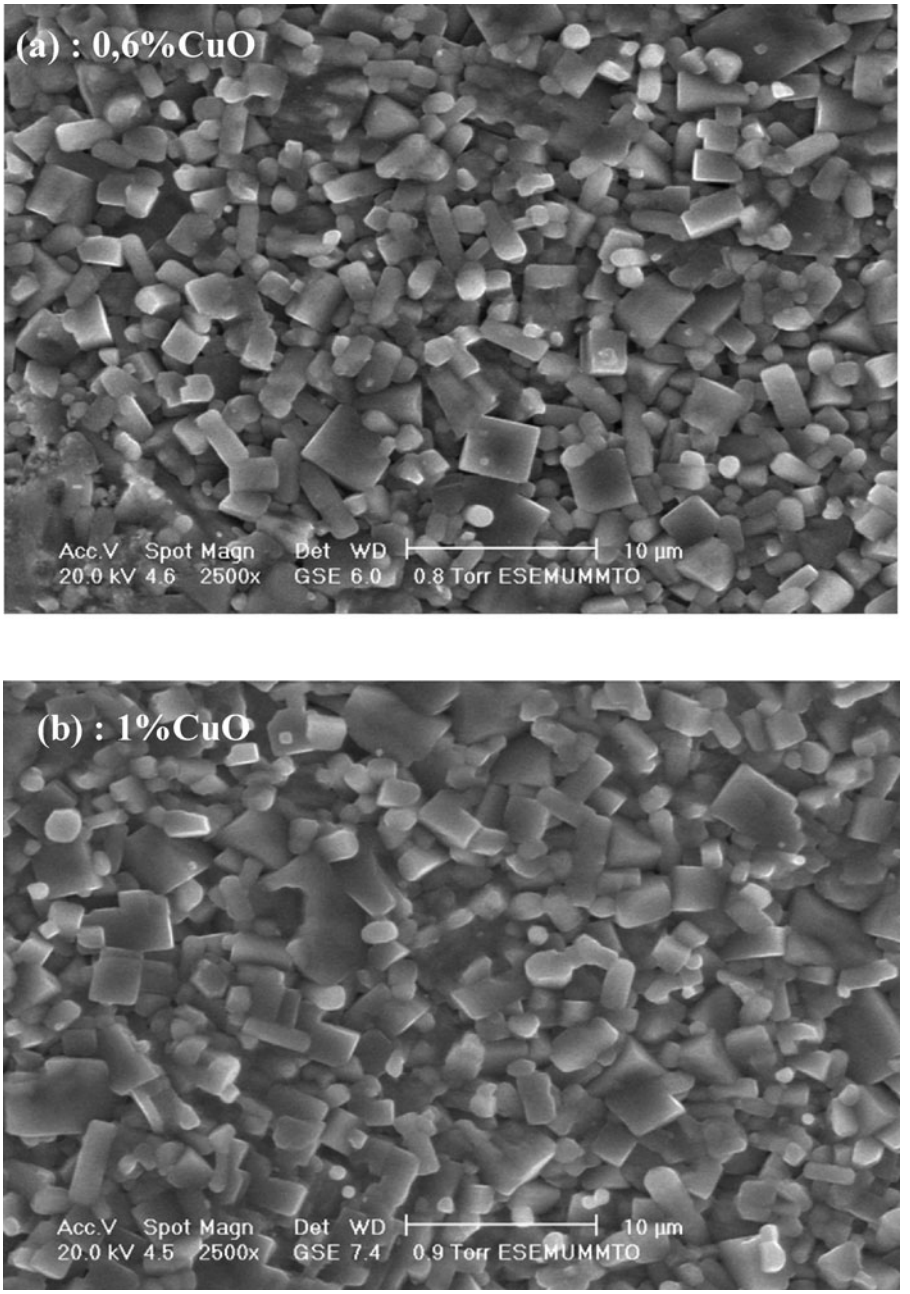

Figure 2. Scanning electron micrographs of fracture for the sintered ceramic.

be well sintered, as shown in Fig. 2(a) and (b). All the ceramics show the formation of large grains is attributed to presence of the liquid phase, which is consistent with the other reports that the formation of large grains is ascribed to the existence of the liquid phase in the KNN-based ceramics [23].

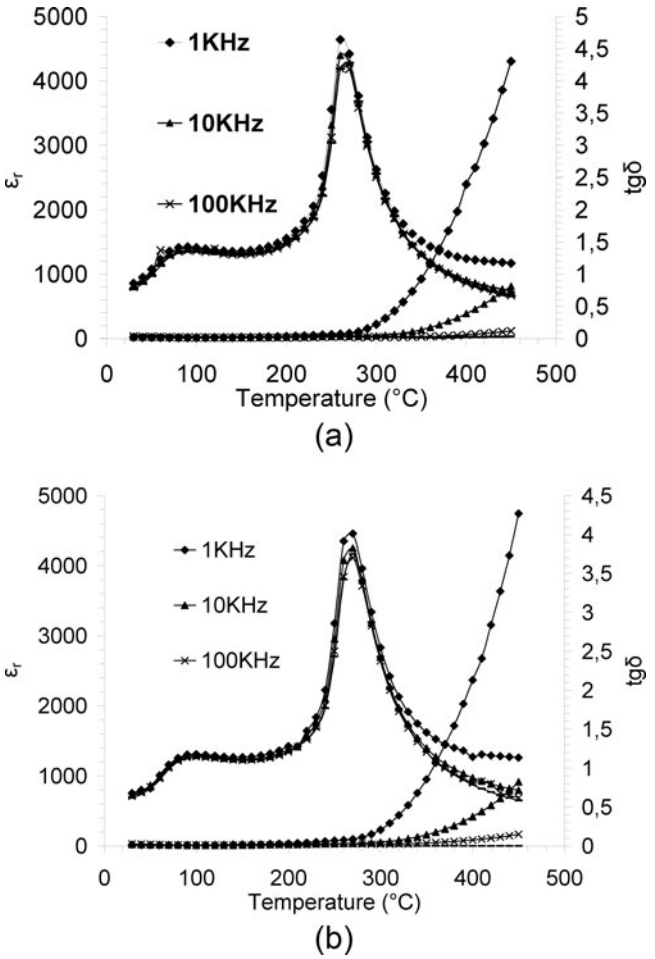

Figure 3. Temperature dependence of permittivity and dielectric loss at different frequency of NKNSLT +xwt.% CuO compositions: (a) x = 0.6 and (b) x = 1.

3.2. Dielectric and Piezoelectric Studies

Fig. 3 shows the temperature dependences of dielectric constant and dielectrics loss for the NKNSLT +xw.%CuO ceramics at different frequency (1kHz, 10 kHz, and 100 kHz). As shown in Fig. 3, there are two phase transition temperatures. For the higher phase transition temperatures, corresponding to tetragonal to cubic phase (Tc), all the ceramics present similar temperatures around 360°C, which suggests that the excess CuO added would not obviously affect the Tc of NKNSLT ceramics [24]. For the lower phase transition temperatures, corresponding to orthorhombic to tetragonal phase ($T_{o\text{-}t}$).

At room temperature, the dielectric loss (tanδ) was lower, and the dielectric constant (ε_r) varied from 800 to 1400. The dielectric loss increases rapidly at higher temperature due to the rapid increase of conductivity. The temperature T_m corresponding to the maximum value of the dielectric constant decreases with increasing frequency. The broadening of the ε_r peaks and the obvious frequency dispersion indicate that NKNSLT +xw.%CuO ceramics present relaxor ferroelectric phenomena.

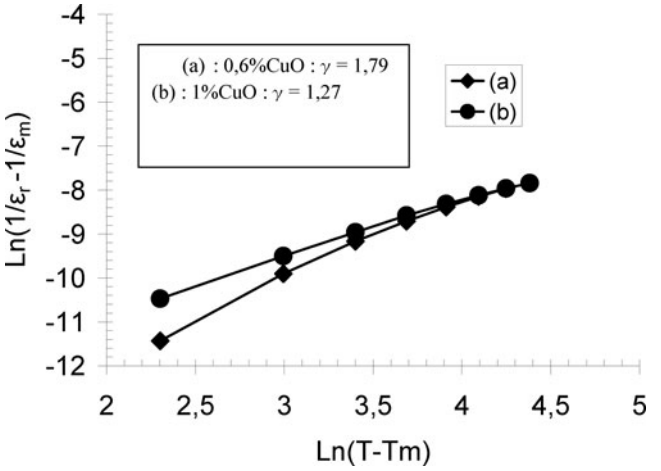

Figure 4. Plots of $\ln((1/\varepsilon_r) - (1/\varepsilon_m))$ vs ln(T - Tm) at 1kHz for of sintered ceramics.

A modified empirical expression proposed by Uchino and Nomura [25] is employed in this work to further characterize the dielectric dispersion and diffuseness of the phase transition:

$$(1/\varepsilon_r) - (1/\varepsilon_m) = A(T - T_m)^{\gamma}$$

where ε_m is the peak value of dielectric constant, and T_m is the temperature at which ε_r value reaches the maximum. The terms γ and A are assumed to be constant, γ value is between 1 and 2. The limiting values $\gamma = 1$ and 2 reduce the expression to the Curie–Weiss law, which is valid for the case of normal ferroelectric, and to the quadratic dependence, which is valid for an ideal relaxor ferroelectric[26], respectively. The logarithmic plots related to this equation for NKNSLT +xw.%CuO compositions are shown in Fig. 4. A linear relationship is observed for two samples. By linear fitting the experimental data to the modified Curie–Weiss law, γ is determined to be 1.27 for NKNSLT +1%CuO, and $\gamma = 1.76$ for NKNSLT +0.6%CuO compositions revealing relaxors ferroelectrics of these ceramics. These results are in accordance with the results of Figs. 3(a) and 3(b).

Fig. 5 shows the P–E hysteresis loops of the NKNSLT +xw.%CuO (with x = 0.6, and 1) ceramics, all the ceramics exhibit a well-saturated P–E hysteresis loop, suggesting that the ceramics have good ferroelectric properties. From the loops Fig. 5, the remnant polarization P_r and the coercive field E_C (indicating the electric field required to zero the polarization) are determined to be near to 7 μC/Cm^2, and 1000V/cm for these compositions, respectivity.

The piezoelectric constant d_{33} and planar electromechanical coefficient k_p also show interesting values. For NKNSLT +1.%CuO compositions, the d_{33} and k_p reach the maximum values, which are 91 pC/N and 23%, respectively. Theses high values reveal the promotion of piezoelectric properties at NKNSLT +1w.%CuO is expected owing to the coexistence region where both the orthorhombic and tetragonal phases exist and thus more possible polarization states. Another possible reason is partly attributed to dense microstructure with high bulk density which can lower the leakage current and enhance the poling process [27].

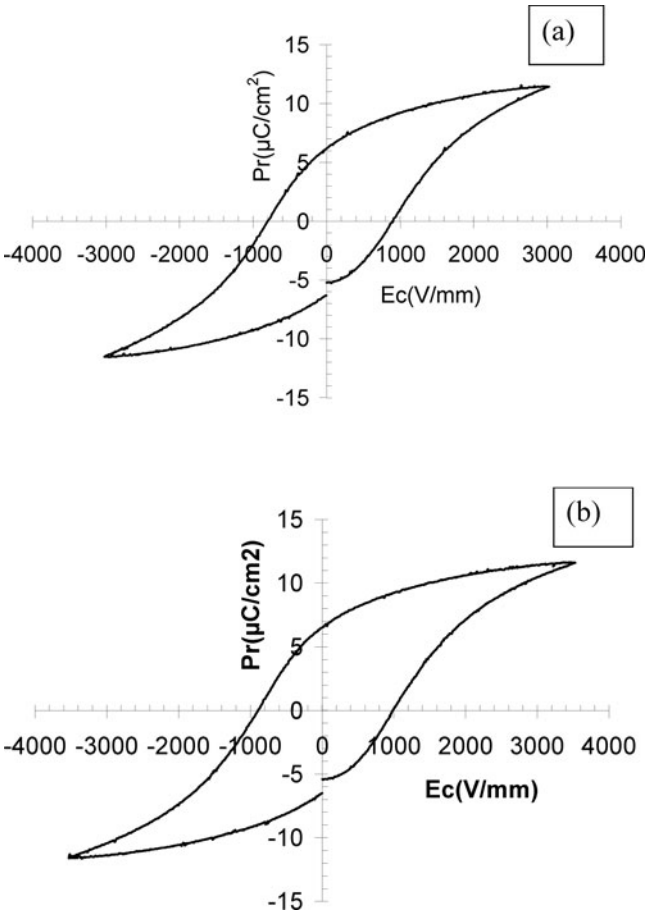

Figure 5. P–E hysteresis loops: (a) NKNSLT +0.6% CuO and (b) NKNSLT +1% CuO.

3.3. Complex Impedance Spectrum Analysis

Impedance spectroscopy (IS) is a relatively new and powerful method of characterizing the electrical properties of materials and their interface with electrodes. It may be used to investigate the dynamics of bound or mobile charge in the bulk or interfacial regions of any kind of solid including ionic or mixed electronic-ionic materials and even insulators [28].The resultant response (when plotted in a complex plane) appears in the form of a succession of semicircles representing contributions due to the bulk, grain boundaries and interfaces. A polycrystalline material usually shows both grain and grain boundary effects with different time constants (relaxation times) leading to two successive semicircles [29]. Electrical properties of a material are often represented in terms of some complex parameters like complex impedance (Z^*), complex admittance (Y^*), complex modulus (M^*), complex permittivity (ε^*) and dielectric loss ($\tan\delta$). These frequency dependent parameters are related to each other by the following relations [30]:

$$\varepsilon* = \varepsilon' + j\varepsilon'' \tag{1}$$

$$Z^* = Z' + jZ'' = (1/jC_0\varepsilon^*\omega) \tag{2}$$

$$Y^* = Y' + jY'' = j\omega C_0 \varepsilon^* \tag{3}$$

$$M^* = M' + jM'' = (1/\varepsilon^*) = j\omega\, C_0 Z^* \tag{4}$$

$$\tan\delta = (\varepsilon''/\varepsilon') = (M'/M'') = (Y'/Y'') = (Z'/Z'') \tag{5}$$

where $\omega = 2¶$, f is the angular frequency, C_0 is the free geometrical capacitance, and $j^2 = -1$. These relations offer wide scope for a graphical analysis of the various parameters under different conditions of temperature or frequency. The useful separation of intergranular phenomena depends ultimately on the choice of an appropriate equivalent circuit to represent the sample properties.

Fig. 6 shows the variation of the real part of impedance (Z') with frequency at various temperatures for both NKNSLT +0.6%CuO and NKNSLT +1%CuO specimens. It is observed that the magnitude of Z' decreases with increase in both frequency and temperature, indicating an increase in ac conductivity with rise in temperature and frequency. The Z' values for all temperatures merge at high frequency. This may be attributed to the increase of ac conductivity with temperature and frequency in the higher frequency region due to the removal of space charge as a result of reduction in barrier height [31]. Further, at low frequency, Z' values decrease with an increase in temperature and show negative temperature coefficient of resistance (NTCR) type behavior similar to that of semiconductors.

Fig. 7 shows the variation of imaginary part of impedance (Z'') with frequency. The plots show that Z'' values attain a peak (Z''_{max}) at all measuring temperatures.

The magnitude of Z''_{max} decreases with temperature indicating decrease in the resistive property of the sample. The value of Z''_{max} shifts to the higher frequencies with increasing temperature, this indicates the occurrence of relaxation in the system [32]. The peak (Z''_{max}) broadening with increase in temperature suggests the presence of temperature dependent electrical relaxation phenomenon in the material. This relaxation process is due to the presence of immobile species at lower temperatures and defects /vacancies at higher temperatures [33].

Fig. 8 shows the complex impedance plot of Z'' vs. Z' (Nyquists plot) for NKNSLT +xw.%CuO at different temperatures. From Fig. 8 it is clear that the semicircular arc shifts towards origin indicating the increase in conductivity of the sample as the temperature increases. All the curves start at the origin, and hence there is no series resistance of the sample. The semicircles have their centers located slightly away from the real axis, indicating the presence of relaxation species with distribution of relaxation times in the sample. Furthermore, the shape of the curve suggests that the electrical response is completely dominated by the bulk properties of the material.

Thus, the electrical properties of NKNSLT + xw.%CuO can be represented by a parallel combination of RC circuits (inset of Fig. 8(a)). The value of R_g (dc resistance) of the materials given in Table 1, was obtained from the intercept of the semicircular an arc on the real axis (Z').The capacitance values of the grains (C_g) have been calculated by this equation: $C_g = 1/R_g.2\pi\ f_{max,}$ where f_{max} is the relaxation frequency of Z'' vs frequency (the value of frequency at Z''_{max} obtained at Fig. 7). The decrease in grain boundary resistance with rise in temperature may be due to the lowering of barrier favouring the increase of mobility of charge carriers that adds to the conduction. The values of grain resistance (R_g) reveal the high value in the case of NKNSLT + 1%CuO. This suggests that the conductivity in the perovskites can be described as an ordered diffusion of oxygen vacancies [34]. These quantities of oxygen vacancies can be decreased by addition of donors; since the donor

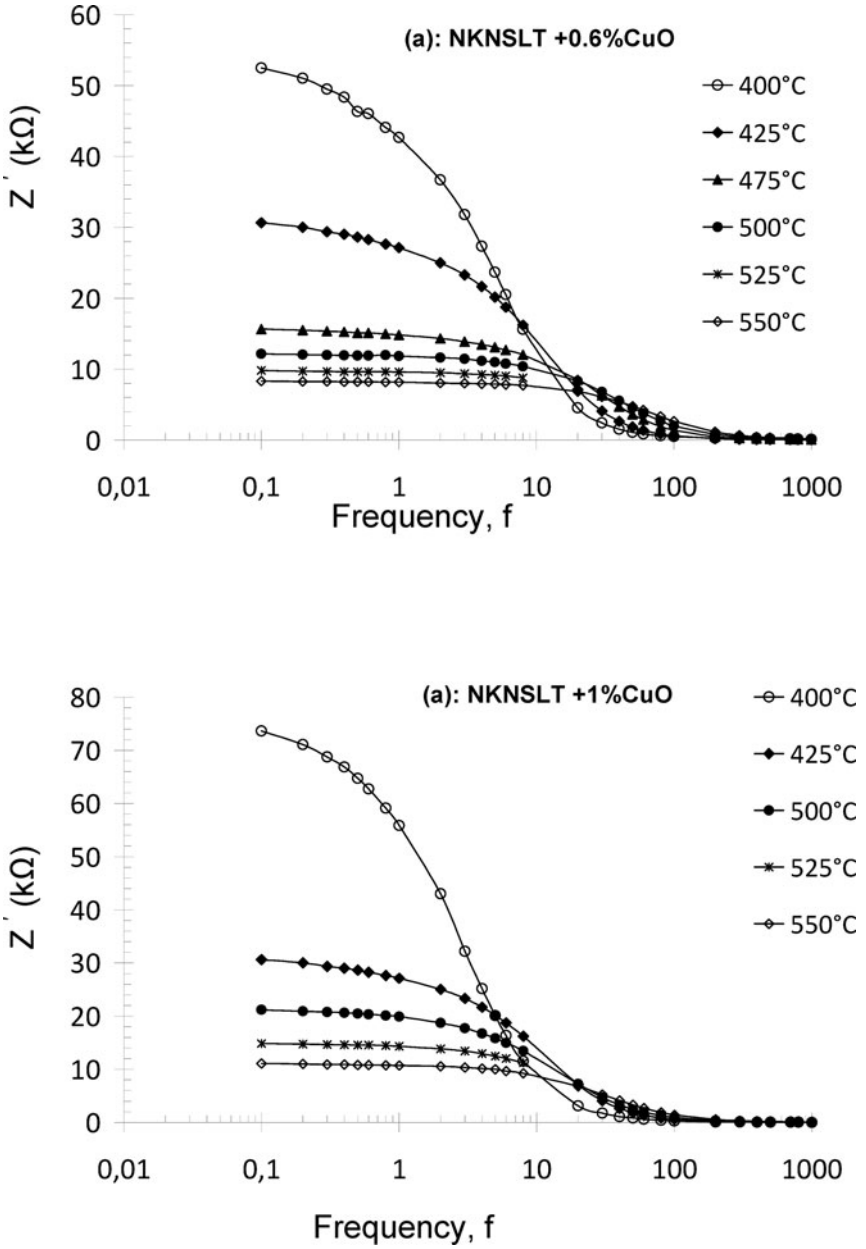

Figure 6. Variation of real part of impedance (Z′) of NKNSLT +xwt.% CuO with frequency at different temperature.

oxide contains more oxygen per cation than the host oxide it replaces [35]. In ours work, the CuO is a donor, and can replace the evaporation of K or Na, it may be expressed by Kroger–Vink notation as:

$$2V'_{Na} + V_o^{\circ\circ} \xrightarrow{Cuo} Cu_{Na}^{\circ} + O_O^x + e'$$

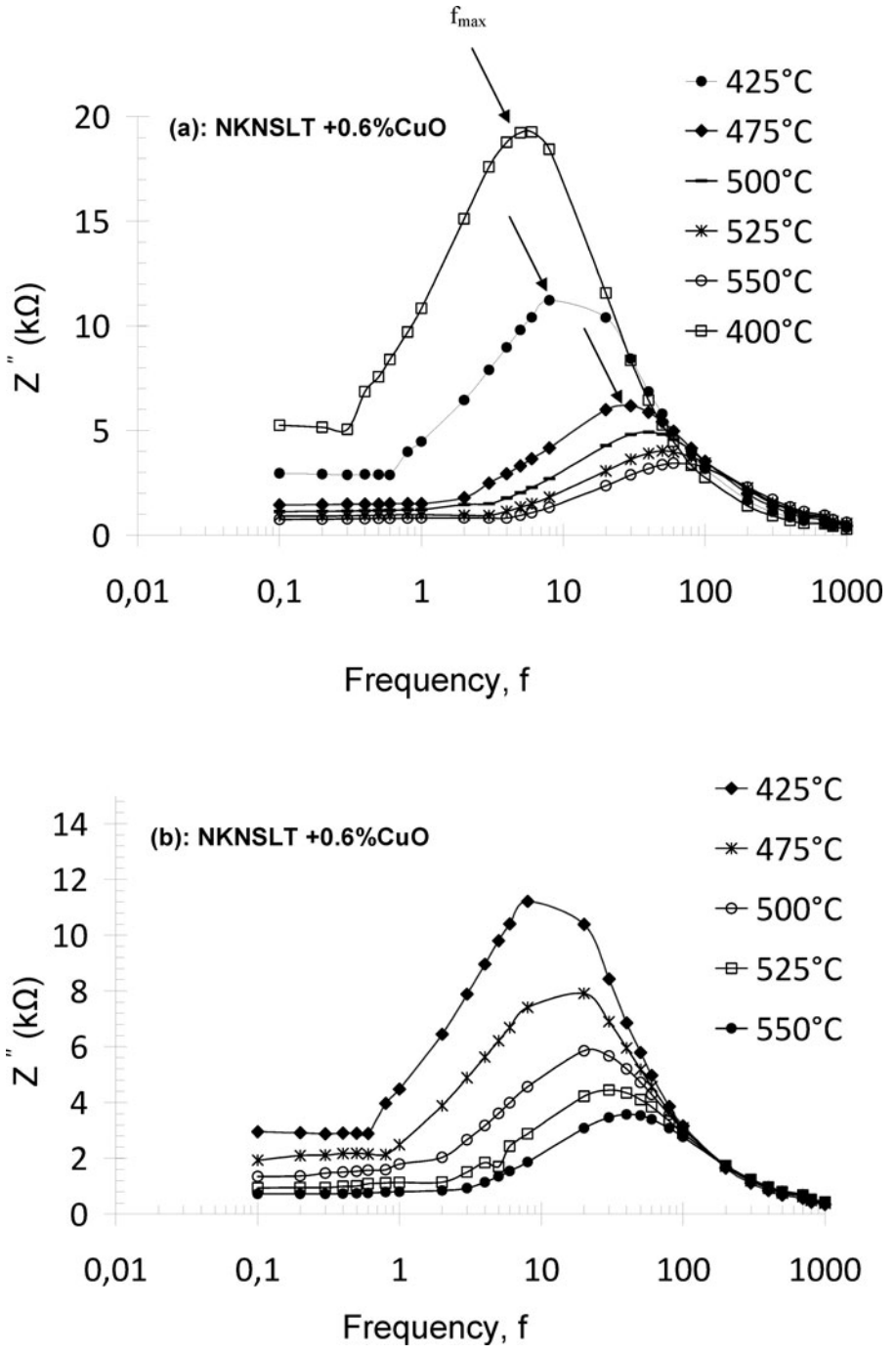

Figure 7. Variation of imaginary part (Z′′) of impedance of NKNSLT +xwt.% CuO with frequency at different temperature.

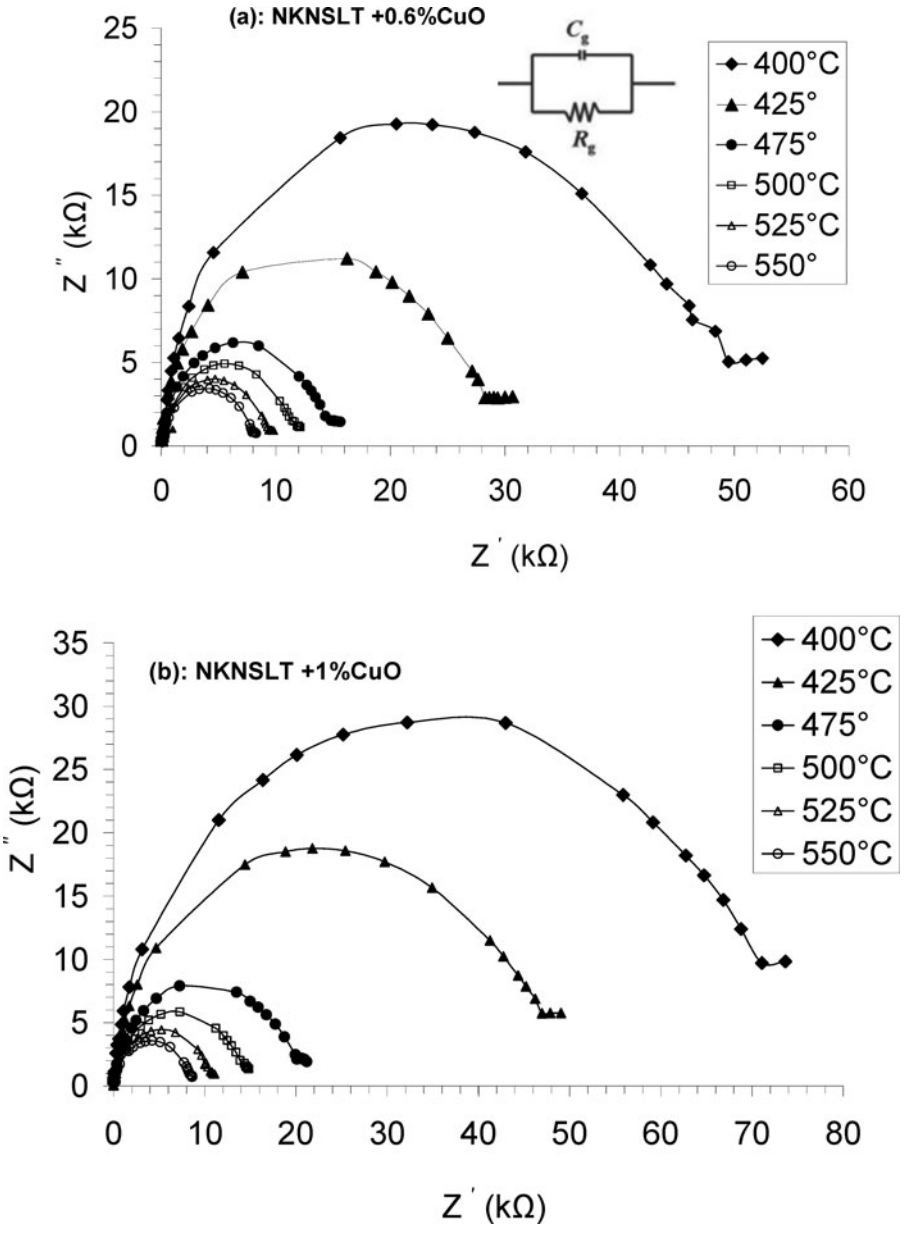

Figure 8. Complex impedance plots (Z′′ vs. Z′) of (a) NKNSLT +0.6%CuO and (b) NKNSLT +1%CuO at different temperature.

$$2V'_k + V_O^{\circ\circ} \xrightarrow{Cuo} Cu_k^{\circ} + O_O^x + e'$$

where, Na^+ or K^+-site vacancy in the structure (noted V'_{Na} and V'_k, respectively), $V_o^{\circ\circ}$ is the presence of oxygen-ion vacancy, e' is the electron released or captured, and Cu^{2+} can replaces the Na^+ or K^+-site vacancy (designated by Cu_{Na}° and Cu_k°, respectively).

Table 1

Grain resistance and capacitance obtained from Nyquist plot (Z″ vs Z′)

	NKNSLT +0.6%CuO		NKNSLT +1%CuO	
Temperature	Rg (Ω)	Cg (F)	Rg (Ω)	Cg (F)
400°C	54000	3,37E-09	80000	5,00E-09
425°C	30000	2,56E-09	50000	4,44E-09
475°C	16000	3,13E-09	24000	3,21E-09
500°C	12500	2,67E-09	16000	3,13E-09
525°C	10000	1,67E-09	12000	2,38E-09
550°C	8000	1,56E-09	9500	2,11E-09

In the consideration of the above reactions, we can note that if the CuO quantity increases, the oxygen vacancy decreases. In this case, the increase substitution of CuO in the solid solutions may decrease the source of oxygen vacancies ($V_o^{\circ\circ}$). Furthermore, the increased activation energy of solid solutions with the increase the CuO content (results cited above), which may be evidence of decreased concentration of oxygen vacancies in the ceramics. As a result, the high value resistivity of NKNSLT + 1%CuO ceramics.

3.4. Electrical Modulus Spectrum Analysis

Complex electric modulus formalism/ analysis gives information on the nature of polycrystalline (homogeneous or inhomogeneous) samples, which can be resolved into bulk and grain boundary effects. It indicates also the electrical phenomenon with the smallest capacitance occurring in a dielectric system [36]. The complex electric modulus (M*) was calculated using The equations: $M' = \omega C$ o Z'' and $M'' = \omega C_o Z'$, $C_o = \varepsilon_o$ A/t, (where ε_o = permittivity of free space, A = area of the electrode surface and t = thickness of the sample). The frequency dependence of the imaginary part of the electric modulus (M″) at different temperatures is shown in Fig. 9. The frequency region below peak maximum

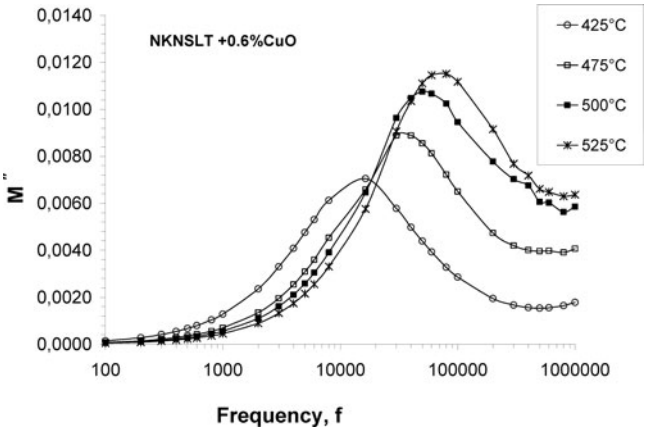

Figure 9. Variation of imaginary part of modulus (M″) with frequency.

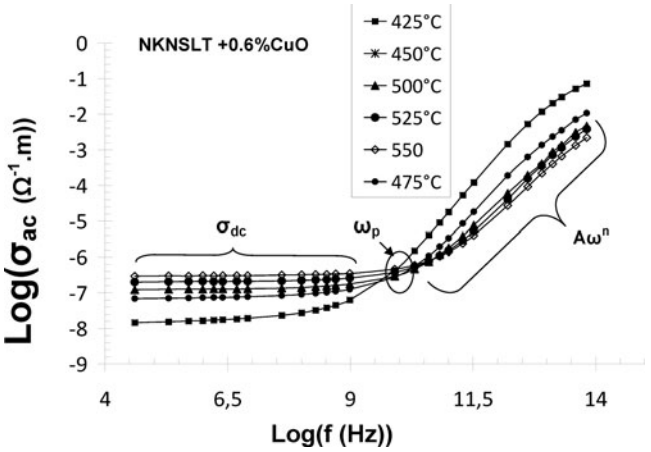

Figure 10. Frequency dependence of ac conductivity vs frequency at different temperatures.

(M′′) represents the range in which the charge carriers are mobile at long distances. At frequencies above peak maximum, the carriers are confined to potential wells and are mobile at short distances [32].

It may be mentioned here that as the samples NKNSLT have been synthesized at high temperature, a slight amount of oxygen loss can occur and it may be expressed by the Kroger-Vink notation [35]:

$$O_O^x = V_O^{\circ\circ} + {}^1/_2\, O_2 + 2e'$$

The formation of oxygen vacancies facilitate the appearance of dipoles formed with an adjacent host ion and enlarge the rattling space available for dipole vibration, which as a consequence leads to the short-range hopping of the ions and gives rise to relaxation.

3.5. Electrical Conductivity Analysis

Fig. 10 shows the variation of ac conductivity (σ_{ac}) with frequency at higher temperatures for NKNSLT +0.6%CuO ceramics. The σ_{ac} was calculated from dielectric data using the following relation: $\sigma_{ac} = d/A.Z'$, where d is the thickness and A is the surface area of the specimen. The Jonscher power law is used to fit the ac conductivity of the material as follows: $\sigma_{ac} = \sigma_{dc} + A\omega^n$ where σ_{dc} is frequency independent conductivity that related to dc conductivity, A is the temperature dependent pre-exponential factor and n is the frequency exponent. The value of n varies between 0 and 1 [37].

Two regions are observed in the conductivity spectrum. The long-range translational hoping conduction in low frequency region gives rise to dc conductivity (σ_{dc}). The frequency dependant short-range translational and localized hoping conduction at high frequency is assigning by $A\omega^n$ term. The frequency at which a change in the slop takes place is known as the "hopping frequency ω_p". The cross over from the frequency independent region to the frequency dependent region shows the onset of the conductivity relaxation, which further indicates the transition from long range hopping to the short-range ionic motion. The onset of conductivity relaxation shifts to higher frequency side with rise in temperature. At low frequency, the σ_{ac} increases with temperature confirming the negative

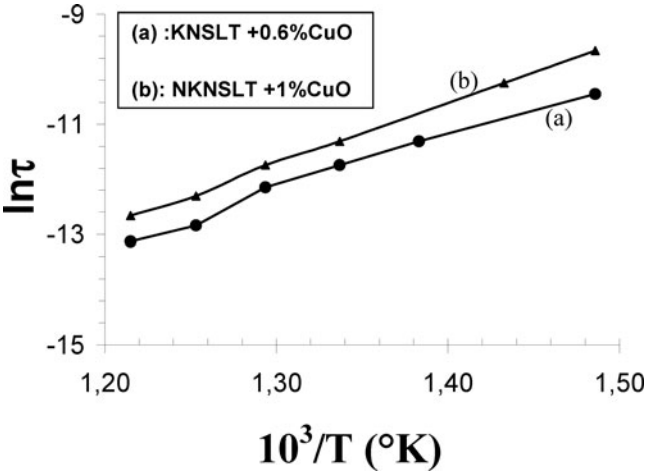

Figure 11. Arrhenius diagram of relaxation times, $\mathrm{Ln}(\tau_{Z''})$ as a function of reciprocal temperature.

temperature coefficient of resistance (NTCR) behaviour that is a typical characteristic of a semiconductor.

The impedance (Z'') vs frequency spectrums were used to evaluate the relaxation time (τ) of the electrical phenomenon occurring in the material at different temperature using the relation: $\tau = 1/\omega = 1/2\pi f_{max}$, where f_{max} is the relaxation frequency (the value of frequency at Z''_{max}).

Fig. 11 shows a typical variation of the relaxation time with inverse of absolute temperature (10^3/T). The activation energy (E_a) was evaluated from the two different slop of the graph using the Arrhenius expression:

$$\tau = \tau_0 \exp(-E_a/kT)$$

where τ_0 is the pre-exponential factor, k is Boltzmann constant and T is the absolute temperature.

The obtained value of activation energy are 0,87 and 0,96 for NKNSLT + 0.6%CuO and NKNSLT +1%CuO compositions respectively, indicates that the conduction in the materials may be due to the oxygen vacancies. At high temperature range, the activation energy for conduction clearly suggested a possibility of formation of vacancies. In perovskite ferroelectric materials, oxygen vacancies are considered as one of the mobile charge carriers and mostly in titanates, niobates and tantalates, ionization of oxygen vacancies creates conduction of electrons, a process which is defined by the Kroger-Vink notation as:

$$O_O^x \rightarrow 1/2O_2(g) + V_O^{\circ\circ} + 2e'$$

Thus excess electrons and oxygen vacancies are formed in the above reduction reaction. The volatility of alkaline element (K and Na) at high temperature during sintering [39], conduct also to the formation of oxygen vacancy, which also noted by the Kroger-Vink notation as:

$$2Na_{Na}^{x} + O^{x}_{O} \rightarrow 2V'_{Na} + V_{O}^{\circ\circ} + Na_2O \nearrow$$

$$2K_{K}^{x} + O^{x}_{O} \rightarrow 2V'_{K} + V_{O}^{\circ\circ} + K_2O \nearrow$$

These electrons ions or oxygen vacancies can be thermally activated, thus enhancing the conduction process. Doubly charged oxygen vacancies are considered to be the most mobile charges in perovskite ferroelectrics and play an important role in conduction [38].

4. Conclusion

Polycrystalline $(Na_{0.52}K_{0.44})(Nb_{0.9}\ Sb_{0.06})O_3$–$0.04LiTaO_3$+xw%CuO ceramics sintered at low temperature and has been studied by a complex impedance spectroscopy technique. Structural and electrical properties of the material have been estimated from impedance data. These results have been expressed in terms of complex impedance spectrum, complex permittivity spectrum, complex modulus spectrum and conductivity spectrum. The compound shows a diffuse type of ferroelectric–paraelectric phase transition having relaxor behaviour. Complex impedance analysis suggests dielectric relaxation to be of polydispersive non-Debye type with a temperature dependent behaviour. Modulus analysis has established the possibility of hopping mechanism for electrical transport process in this material. The activation energy for conduction (E_a) of the material is found to be near 1 eV, which is attributed to the energy required for the motion of oxygen vacancies confirming the conductivity is due to the movements of oxygen vacancies in the material.

References

1. K. Uchino, *Ferroelectric Devices*, Marcel Dekker, Inc., New York, USA, 2000.
2. J. Kulawik, D. Szwagierczak, and B. Groger, Investigations of properties of ceramic materials with perovskite structure in chosen electronic applications. *Bull. Pol. Ac.: Tech.* **55**, 293–297 (2007).
3. M. D. Maeder, D. Damjanovic, and N. Setter, Lead free piezoelectric materials. *J. Electroceram.* **13**, 385–392 (2004).
4. Y. Saito, H. Takao, T. Tani, T. Nonoyama, K. Takatori, T. Homma, T. Nagaya, and M. Nakamura, *Nature* **432**, 84 (2004).
5. B. Q. Ming, J. F. Wang, P. Qi, and G. Z. Zang, *J. Appl. Phys.* **101**, 054103 (2007).
6. Z. P. Yang, Y. F. Chang, and L. L. Wei, *Appl. Phys. Lett.* **90**, 042911 (2007).
7. D. M. Lin, K. W. Kwok, and H. L. W. Chan, *J. Phys. D: Appl. Phys.* **40**, 6060 (2007).
8. E. K. Akdogan, K. Kerman, M. Abazari, and A. Safari, *Appl. Phys. Lett.* **92**, 112908 (2008).
9. J. G. Wu, T. Peng, Y. Y. Wang, D. Q. Xiao, J. M. Zhu, Y. Jin, J. G. Zhu, P. Yu, L. Wu, and Y. H. Jiang, *J. Am. Ceram. Soc.* **91**, 319 (2008).
10. R. E. Jaeger and L. Egerton, *Am. Ceram. Soc.* **45**, 209–13 (1962).
11. L. Egerton and D. M. Dillom, *J. Am. Ceram. Soc.* **42**, 438–42 (1959).
12. Z. S. Ahn and W. A. Schulze, *J. Am. Ceram. Soc.* **70**, 18–21 (1987).
13. J. H. Yoo, D. H. Kim, Y. H. Lee, I. H. Lee, S. H. Lee, I. S. Kim, *et al. Integr. Ferroelectr.* **105**, 18 (2009).
14. D. Gao, K. W. Kwok, D. Lin, and H. L. W. Chan, *J. Mater. Sci.* **44**, 2466–70 (2009).
15. L. Wu, D. Xiao, J. Wu, Y. Sun, D. Lin, J. Zhu, *et al. J. Eur. Ceram. Soc.* **28**, 2963–8 (2008).
16. Y. Lee, B. Seo, Y. Oh, J. Yoo, I. Kim, and J. Song, *J. Korean. Phys. Soc.* **57**, 959 (2010).
17. H. Y. Park, C. W. Ahn, K. H. Cho, S. Nahm, H. G. Lee, H. W. Kang, D. H. Kim, and K. S. Park, *J. Am. Ceram. Soc.* **90**, 4066 (2007).

18. Y. Saito, H. Takao, I. Tani, T. Nonoyama, K. Takatori, T. Homma, T. Nagaya, and M. Nakamura, *Nature* **432**, 84 (2004).
19. K. Goda and M. Kuwabara, *Ceram. Trans.* **22**, 503 (1991).
20. O. Bidault, P. Goux, M. Kchikech, M. Belkaoumi, and M. Maglione, *Phys. R*
21. C. Ang, Z. Yu, and L. E. Cross, *Phys. Rev. B* **62**, 228 (2000).
22. Y. Guo, K. Kakimoto, and H. Ohsato, *Solid State Commun.* **129**, 279–284 (2004).
23. Y. Zhen and J. F. Li, Normal sintering of (K, Na)NbO_3 -based ceramics: influence of sintering temperature on densification, microstructure, and electrical properties. *Journal of the American Ceramic Society* **89**, 3669 (2006).
24. Xuming Pang, Jinhao Qiu, Kongjun Zhu, and Yang Cao, "Effects of Sb content on electrical properties of lead-free piezoelectric ($K_{0.4425}Na_{0.52}Li_{0.0375}$) ($Nb_{0.9625-x}Sb_xTa_{0.0375}$)$O_3$ ceramics" *Ceramics International* **38**, 1249–1254 (2012).
25. K. Uchino and S. Nomura, *Ferroelect. Lett. Sect.* **44**, 55 (1982).
26. D. Viehland, M. Wuttig, and L. E. Cross, *Ferroelectrics* **120**, 71 (1991).
27. R. C. Chang, S. Y. Chu, Y. F. Lin, C. S. Hong, P. C. Kao, and C. H. Lu, *Sens. Actuators A* **138**, 355 (2007).
28. J. R. Macdonald, *Impedance Spectroscopy: Emphasizing Solid State Material and Systems*, Wiley, New York, 1987 (ch. 2 and ch. 4).
29. B. Behera, P. Nayak, and R. N. P. Choudhary, *J. Alloys Comp.* **436**, 226 (2007).
30. Prasun Ganguly, A. K. Jha, and K. L. Deori, *Solid State Comm.* **146**, 472–477 (2008).
31. K. Lily, K. Kumari, R. N. P. Prasad, and Choudhary, *J. Alloys Compd.* **453**, 325 (2008).
32. B. Behera, P. Nayak, and R. N. P. Choudhary, *Mat. Res. Bull.* **43**, 401 (2008).
33. Balgovind Tiwari and R. N. P. Choudhary, *J. of Phy. and Chem. of solids* **69**, 2852–2857 (2008).
34. J. R. Macdonald, *Impedance Spectroscopy: Emphasizing Solid Materials and Systems*, Wiley, New York, 1987, pp. 191–237.
35. S. Selvasekarapandian and M. Vijaykumar, *Mater. Chem. Phys.* **80**, 29 (2003).
36. F. A. Kroger and H. Vink, *J. Solid State Phys.* **3**, 307 (1956).
37. A. K. Jonscher, Dielectric relaxation in solids. *J. Phys. D: Appl. Phys.* **32**, R57 (1999).
38. N. Hirose and A. R. West, *J. Am. Ceram. Soc.* **79**, 1633 (1996).